ARMY RESEARCH LABORATORY

Wide-Angle X-ray Scattering Characterization of the Morphology of Nylon 6 6 Obturator Materials

by Frederick L. Beyer and Christopher Ziegler

ARL-TR-3270 August 2004

NOTICES

Disclaimers

The findings in this report are not to be construed as an official Department of the Army position unless so designated by other authorized documents.

Citation of manufacturer's or trade names does not constitute an official endorsement or approval of the use thereof.

Destroy this report when it is no longer needed. Do not return it to the originator.

Army Research Laboratory
Aberdeen Proving Ground, MD 21005-5069

ARL-TR-3270 **August 2004**

Wide-Angle X-ray Scattering Characterization of the Morphology of Nylon 6 6 Obturator Materials

Frederick L. Beyer and Christopher Ziegler
Weapons and Materials Research Directorate, ARL

Report Documentation Page

Form Approved
OMB No. 0704-0188

1. REPORT DATE *(DD-MM-YYYY)*	2. REPORT TYPE	3. DATES COVERED (From - To)
August 2004	Final	December 2003–February 2004

4. TITLE AND SUBTITLE
Wide-Angle X-ray Scattering Characterization of the Morphology of Nylon 6 6 Obturator Materials

5a. CONTRACT NUMBER

5b. GRANT NUMBER

5c. PROGRAM ELEMENT NUMBER

6. AUTHOR(S)
Frederick L. Beyer and Christopher Ziegler

5d. PROJECT NUMBER
AH42

5e. TASK NUMBER

5f. WORK UNIT NUMBER

7. PERFORMING ORGANIZATION NAME(S) AND ADDRESS(ES)
U.S. Army Research Laboratory
ATTN: AMSRD-ARL-WM-MA
Aberdeen Proving Ground, MD 21005-5069

8. PERFORMING ORGANIZATION REPORT NUMBER
ARL-TR-3270

9. SPONSORING/MONITORING AGENCY NAME(S) AND ADDRESS(ES)

10. SPONSOR/MONITOR'S ACRONYM(S)

11. SPONSOR/MONITOR'S REPORT NUMBER(S)

12. DISTRIBUTION/AVAILABILITY STATEMENT
Approved for public release; distribution is unlimited.

13. SUPPLEMENTARY NOTES

14. ABSTRACT
Two polyamides, both nylon 6 6, were characterized by wide-angle x-ray scattering (WAXS) for variations in morphology that would account for observed differences in mechanical properties. Both materials were found to be macroscopically isotropic, consisting almost entirely of lamellae composed of α_p sheets. No evidence of β_p phase material was found, but both materials showed some evidence of the presence of the nonequilibrium γ (pseudo-hexagonal) phase. The blank provided, made of the first material, DuPont Zytel 101, was found to be highly uniform in morphology. The part provided, made of the second material, Zytel 42A, was found to be nonuniform, with WAXS data indicating a change in the aspect ratio of the crystalline lamellae throughout the part. This change was a likely source of differing mechanical behaviors, although differences in molecular weight and polydispersity have not been eliminated. Changes in processing were recommended as a means to improve the mechanical behavior of the samples.

15. SUBJECT TERMS
nylon 6 6, x-ray scattering, morphology, WAXS, XRD, Zytel

16. SECURITY CLASSIFICATION OF:			17. LIMITATION OF ABSTRACT	18. NUMBER OF PAGES	19a. NAME OF RESPONSIBLE PERSON
a. REPORT	b. ABSTRACT	c. THIS PAGE			Frederick L. Beyer
UNCLASSIFIED	UNCLASSIFIED	UNCLASSIFIED	UL	26	19b. TELEPHONE NUMBER (*Include area code*) 410-306-0893

Contents

List of Figures

List of Tables

INTENTIONALLY LEFT BLANK.

1. Introduction

The crystal structures of polyamides have been very intensively studied and are well understood. The early works continue today as the basic foundation of our current understanding of the nature of the crystal structure of nylon 6 6 (*1*, *2*). It was found that the spherulitic structure observed was composed of chain-folded lamellae, which are in turn composed of stacks of crystalline sheets. The sheets are held together by van der Waals interactions. Bunn and Garner (*1*) proposed two triclinic structures, α and β, for the crystalline domains which form the sheets, where the α structure contains one chain per unit cell, and the β structure contains two. The crystal unit cell dimensions are given in table 1. The formation of these specific structures is required by the formation of hydrogen bonds between the carbonyl and amide groups in neighboring molecules (*3*).

Table 1. Crystal phase unit cells and dimensions for nylon 6 6 (*3*).

Phase	Unit Cell	a (nm)	b (nm)	c (nm)	α (°)	β (°)	γ (°)
α_p	Triclinic	0.490	0.525	1.73	50	77	64
β_p	Triclinic	0.490	0.801	1.73	90	77	66

In addition to the equilibrium α and β phases, a nonequilibrium "pseudohexagonal" (γ) phase was also found (*4*), occurring at high temperatures only. As a sample is heated, the equilibrium α and β structures gradually merge until, at the Brill transition temperature, T_B, only the γ phase is left. The γ structure is triclinic, but appears to be hexagonal when viewed from a specific crystallographic direction (*5*). The Brill transition has been reported at temperatures between 170 and 220 °C, significantly below the melting temperature, T_M, of nylon 6 6. The melting temperature of nylon 6 6 is reported to vary from 250 to 272 °C (*2*, *3*, *6*), presumably depending on molecular weight and thermal history.

Finally, it has been found that the sheets formed by polyamides are "pleated," denoted by a subscript "p" (*1*, *3*). This also results from the necessity of the carboxyl-amide hydrogen bond for stability. In effect, neighboring chains are offset slightly. This motif is repeated, in the α_p structure, producing a 42° offset between the polymer chain axis and the lamellar normal. In the β_p phase, the offset alternates direction between molecules, resulting in no offset with the lamellar normal.

Using wide-angle x-ray scattering (WAXS), it is possible to distinguish between the different crystal structures, under certain conditions. In this case, the α_p and β_p structures are similar enough that in the absence of single crystal diffraction patterns, it is not possible to distinguish one from the other. The characteristic reflections of the α_p structure appear at 0.440 and

0.371 nm and correspond to the (100) reflection and a sum of the (010) and (110) reflections in the case of the α_p phase, respectively. Figure 1 shows a typical powder-type diffraction pattern for nylon 6 6 that has been indexed on the assumption that it is composed of 100% α_p phase. The 0.440-nm reflection corresponds to the interchain, intrasheet periodicity, while the 0.371-nm reflection corresponds to the intersheet periodicity. The β_p structure gives rise to characteristic reflections at nearly the same spacings, but corresponding to the (100) and a sum of the (020) and (120) planes. Table 2 summarizes the interplanar spacings for the important reflections of both the α_p and β_p phases (*3*, *7*).

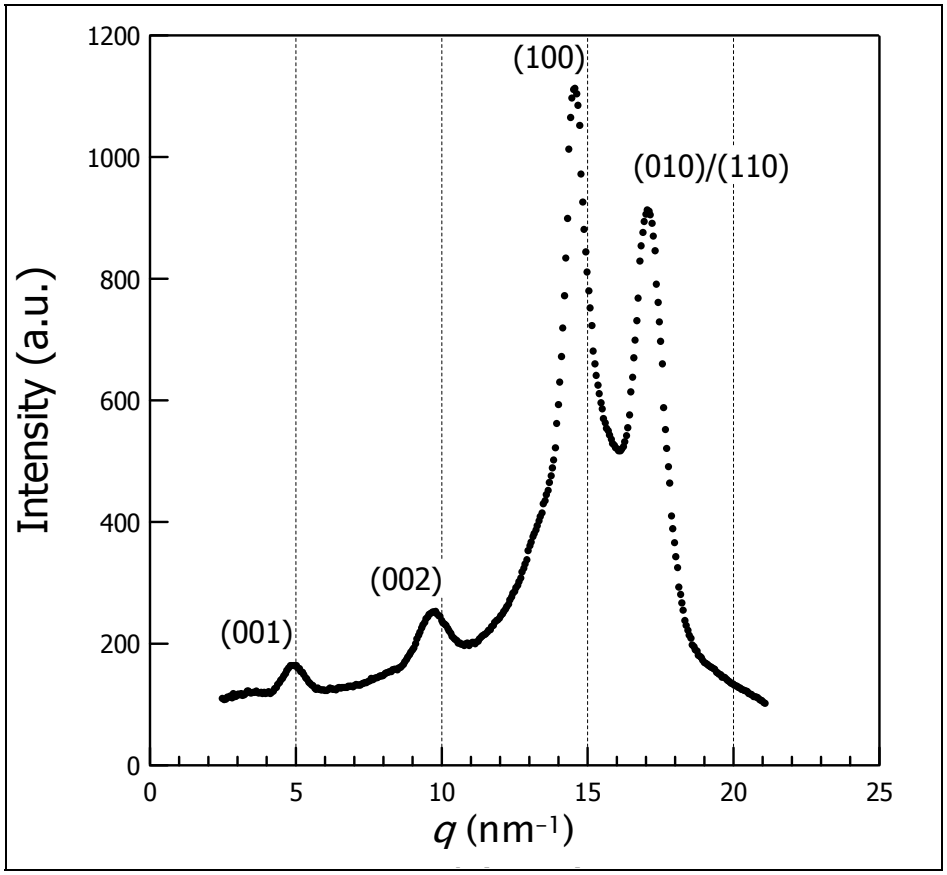

Figure 1. A typical set of one-dimensional (1-D) (powder-type) WAXS data from a nylon 6 6 sample. The four reflections are labeled to indicate the corresponding crystalline plane (in the case of the 100 and 010/110 reflections) or Bragg reflection arising from lamellar stacking (001 and 002).

To distinguish between α_p and β_p, one must be able to tilt the individual crystal in question until the incident beam is parallel to the chain axis. Not only are the differences in the dimensions of the crystalline unit cells more pronounced, but the tilt angle from the lamellar normal is significantly different between the two structures (42° for α_p and 13° for β_p). The γ structure, which is not normally observed at temperatures significantly below T_B, is readily distinguished from α_p and β_p by a characteristic reflection at 0.42 nm. Finally, the period of the stacks of

Table 2. Interplanar spacing and scattering vectors (q) for the characteristic Bragg reflections from the two equilibrium phases of nylon 6 6, calculated using the data in table 1.

Phase	Reflection	Interplanar Spacing (nm)	q (nm^{-1})
α_p	(001)	1.32	4.76
	(002)	0.660	9.52
	(100)	0.439	14.3
	(010)	0.370	17.0
	(110)	0.361	17.4
β_p	(001)	1.68	3.75
	(002)	0.838	7.50
	(100)	0.434	14.5
	(020)	0.364	17.3
	(120)	0.363	17.3

lamellae that occur in the bulk material generates reflections observed at lower angles, typically 1.3 and 0.65 nm.

In this study, two commercial polyamides (both nylon 6 6), DuPont Zytel 42A and Zytel 101, were studied to determine possible causes for the increase incidence of mechanical failure of a projectile obturator when the part was made from 42A rather than 101. The samples were characterized using WAXS in a manner designed to test for changes in morphological structure that might account for the observed change in performance.

2. Experimental

Two nylon 6 6 materials were received for morphological characterization. The specimens were large cylindrical blocks of DuPont Zytel 101 and Zytel 42A. The sample of 101 provided was a blank hollow cylinder ~4 inches in diameter, with a hollow core ~1.5 inches in diameter. The sample of 42A provided was an actual part that had been milled from a blank of the same dimensions as the sample of 101. While the exact processing conditions under which the parts were made from either material are proprietary, it is understood that the nylons were dried and then processed following the recommendations provided by DuPont. The melt temperature was in excess of 260 °C (500 °F), and the residence time in the extruder was minimized. The materials, in the form of hollow cylinders as previously described, were then annealed differently. The 101 material was annealed in a circulating oil bath at 231.7 °C (449 °F), then allowed to slowly cool in the bath. The 42A material was annealed in large metal tubes filled with a nitrogen atmosphere at 231.7 °C (449 °F), then also allowed to slowly cool in the oven. The total annealing time was the same for both processes (around 24 hr). The exact heating and

cooling steps and times are proprietary. In the manufacturing process, the blanks are machined to produce the final obturator part.

Sections were cut from each part to allow for characterization of morphology in the bulk material. Cuts were made along the radial direction from the inner surface of the part to the outer surface of the parts. Large sections were rough-cut from the parts using a band saw. The final samples for characterization were cut using a wet saw with a diamond blade. The 101 sample was cut to 0.54-mm thickness, and the 42A was cut to 0.30-mm thickness. Each specimen was divided into seven areas along the radial direction of the part. As shown in figure 2, the locations were labeled "1" through "7," with "1" being adjacent to the inner surface of the original part, "7" being near the edge of the outer circumference of the piece, and location "4" at the center. Each location was marked on the sample to ensure reproducibility.

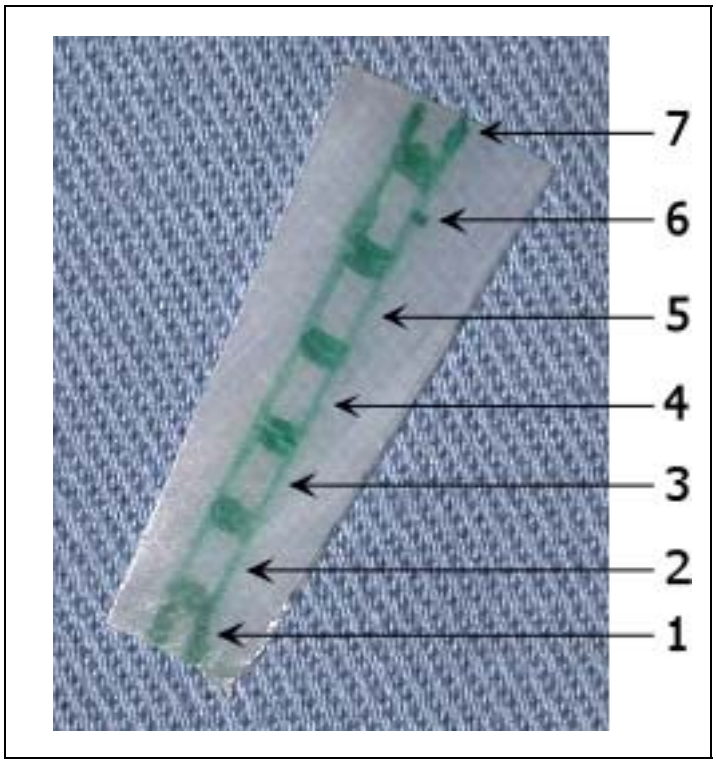

Figure 2. A picture of a section of the nylon 6 6 materials provided. The green markings allow reproducible measurement of properties from different locations in the sample.

WAXS was used to characterize the morphology of the cut sections. A Bruker Hi-Star two-dimensional (2-D) area detector was used with a 3-circle (fixed χ) goniometer platform to collect WAXS data. A Rigaku UltraX18 rotating Cu anode source, operated at 40 kV and 20 mA, was used to generate radiation, which was monochromated to $\lambda = 0.15418$ nm using pyrolytic graphite. The sample-to-detector distance was 6.05 cm, and 0.5-mm, collimation was used. Later characterization was carried out with 0.3-mm collimation (at 60 mA), and at varying

sample-to-detector distances. All data were corrected for detector sensitivity and spatial distortions. The corrected data, which were uniformly isotropic, were azimuthally averaged for presentation and characterization as intensity as a function of the magnitude of the scattering vector, q, where $q = 4\pi \cdot \sin(\theta)/\lambda$. The real space dimension of a given reflection is simply $2\pi/q$. All peak values were obtained using peak fitting techniques and Igor Pro, Version 4.0.7. Simple peak fits were accomplished using the sum of a Gaussian peak with a variable slope linear background fit. Complex fits were accomplished using the multiple peak fitting package within Igor Pro. In those cases, peaks were added based on prior understanding of typical nylon 6 6 morphological features. Peak positions and amplitudes were allowed to vary freely, although some discretion was used to discard implausible fits. Background noise was fitted using a cubic polynomial (not described).

3. Results and Discussion

Figure 3 shows a typical 2-D diffraction pattern collected from sample 101A. All the data collected for both materials were, in overall appearance, nearly indistinguishable from these data. Because these data were all isotropic, showing no evidence of diffraction from individual crystallites, all the 2-D data was azimuthally averaged for interpretation.

Figure 4 shows the individual 1-D data collected from the 101. The data from the seven different locations have been offset for clarity. The expected reflections are observed. A simple fit to the (100) peak was not possible because the shape was not Gaussian, implying that contributions from multiple reflections were included. To further emphasize the uniformity of the scattering data obtained from the 101 samples, figure 5 shows the seven sets of data presented in figure 4, collapsed into a single curve. No variations in the shape, intensity, position, or breath of the four main reflection curves are evident. Figure 6 shows the WAXS data from location 1 (inner surface) of the 101 along with the peak fitting data generated using Igor Pro. Table 3 lists the peaks used to create the fit in figure 6, along with their amplitude, position (in nm^{-1}), and width. Gaussian peak forms were used for all peaks.

Figure 7 shows seven sets of data collected from the sections made of the nylon 42A part provided. The data are vertically offset for clarity, and it can be seen that there is a difference in the relative peak intensities between the data sets collected from the inner surface of the part (location 1) and the rest of the sample. Additionally, figure 8 shows the data sets from locations 1, 4, and 7 collapsed as nearly as possible into a single curve. Unlike the data in figure 5 from the 101 material, significant variations are seen, indicating that the morphology formed in this part is not uniform. Peak fitting was performed on the WAXS data collected from 42A locations 1, 4, and 7, and the results are shown graphically in figures 9–11 and tabulated in table 4.

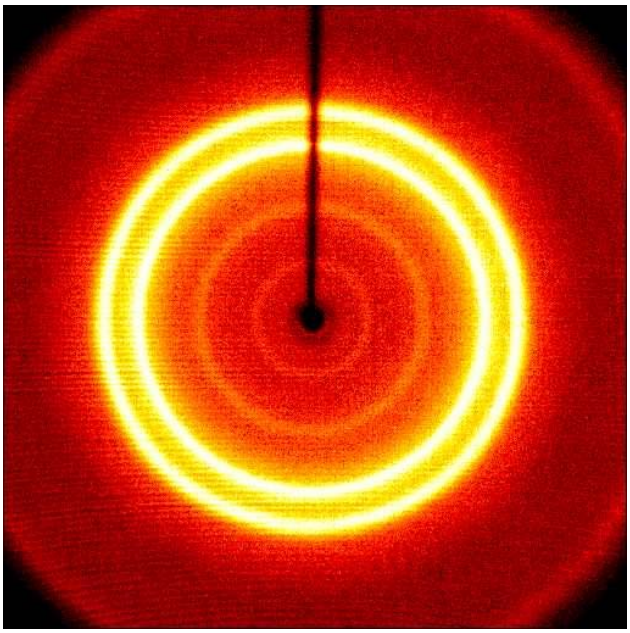

Figure 3. A typical 2-D WAXS data set for nylon 6 6, from the center of the Zytel 101. The isotropic nature of the sample is clear from the solid rings. The two weak inner reflections are from the stacking of lamellae, while the two strong outer rings are the characteristic (100) and (010)/(110) reflections.

The critical, immediate goal of this work was to determine if there were morphological differences between the two nylon 6 6 materials provided: DuPont Zytel 42A and Zytel 101. Morphological differences would contribute to different physical properties that may have contributed to higher failure rates for the obturator parts made from 42A. In the simplest terms, there are substantial differences in the morphologies as characterized by WAXS, and these are significant enough to account for the different observed behaviors.

The 101 material is very homogeneous in morphology, as shown clearly in figure 5 from the inner surface of the blank to the outer surface of the blank. Very slight variations on the peak intensities can be observed in figure 5, but these are well within the uncertainties of the data collection process because no corrections to the raw data were made for sample thickness, transmission, secondary scattering, or background scattering. Overall, the uniformity of the data in figure 5 is remarkable. The 42A material is not homogeneous, as can be seen in figure 8. Some features again cannot be clearly ascribed to changes in morphology, such as the change in the relative intensities of the (002) peaks between locations 1, 4, and 7; these may be attributed to changes in sample thickness, for example. And, the positions of the peaks do not change, indicating that the crystalline phase formed is most likely unchanged. A change was observed, though, in the relative intensities of the two characteristic nylon 6 6 peaks, at ~14.5 nm^{-1} and 17 nm^{-1}, indicating a change in the size and shape of the crystallites that are present.

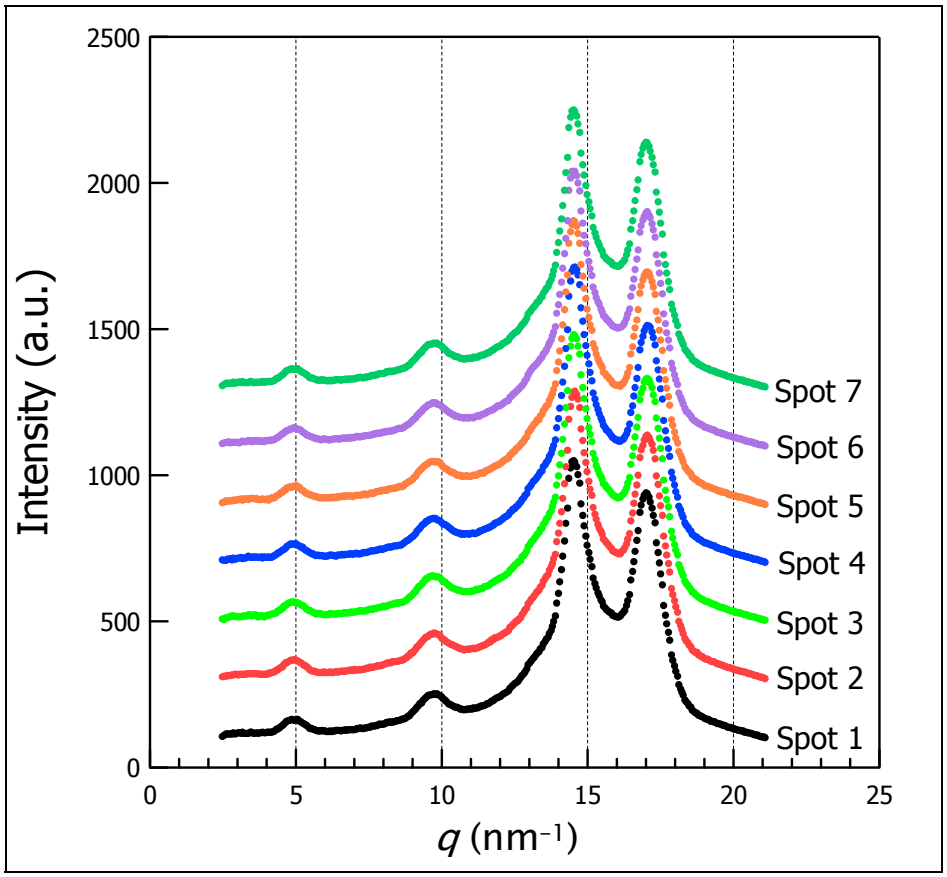

Figure 4. Two-dimensional WAXS data collected at seven different locations from the Zytel 101 material. The typical reflections are very strong and distinct.

The (100) peak is caused by coherent scattering between adjacent polymer chains within the crystalline sheets (interchain, intrasheet scattering). The (010) and (110) peaks arise from intersheet scattering. The relative intensities of these two characteristic peaks shifts with radial position in the 42A part, as seen in figures 9–11, and in the amplitudes of the (100), (010), and (110) peaks, derived from peak fitting. Strong, sharp reflections indicate large, well-refined structures, while weaker, broadened reflections indicate structures that are generally less well-ordered or smaller (*8*, *9*). Closer examination of the peak fitting data shows that the widths of the fitted peaks are essentially constant, with the exception of the (010) peak at location 1, which is ~10% less than at locations 4 and 7. More striking is the significant change in intensity (amplitude) of the (110) reflection in moving from location 1 out to location 7, by more than 50%. The (100) reflection also strengthens from location 1 to 7 by ~20%. These changes indicate that the α_p sheets are becoming larger in size, but that the stacks of sheets (which comprise the lamellae) are becoming smaller as one moves radially outward through the sample. In terms of the lamellae, a likely interpretation of these data is that the lamellae are becoming longer and narrower, but not thinner, as one moves radially from location 1 to 7.

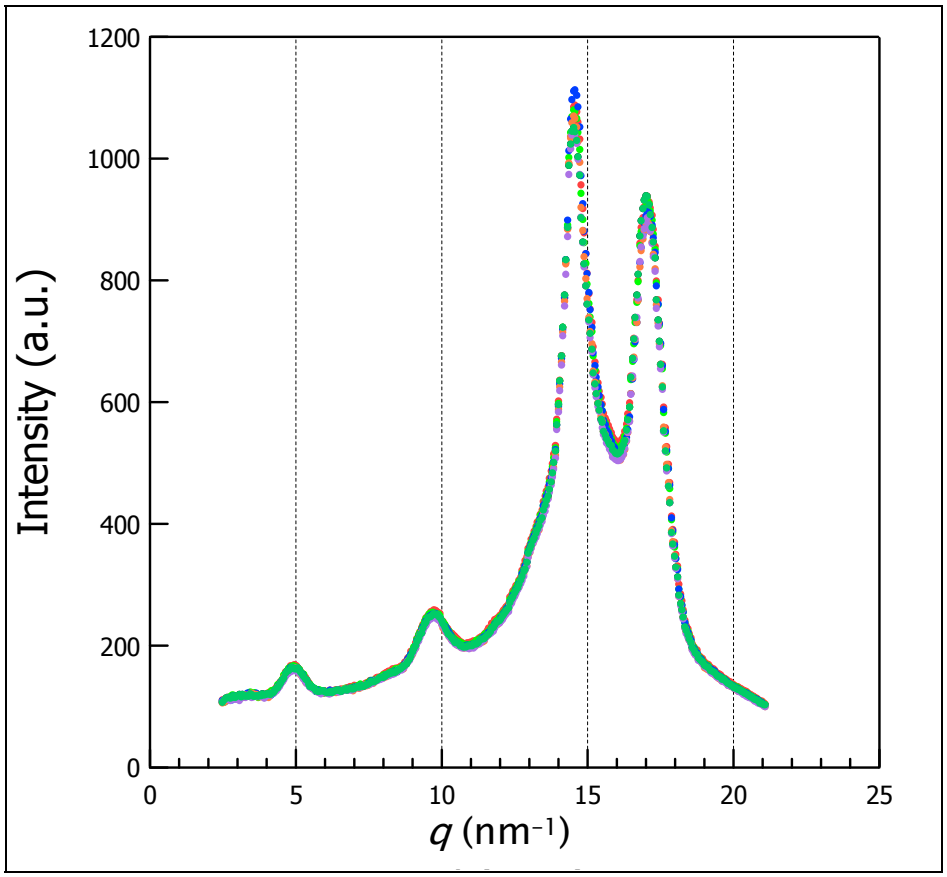

Figure 5. Seven sets of WAXS data from the Zytel 101 material, collapsed into a single curve. Any significant differences in the data would be immediately apparent in this view, but the data show remarkable uniformity, indicating a nearly homogeneous morphology.

These changes in morphology are significant and can be expected to have an impact on mechanical properties. If all other parameters, such as thermal history or molecular weight distribution, were constant, a good strategy to use to improve the performance of the 42A would be to change the annealing process to allow adequate time for the equilibrium morphology to develop throughout the part. In this case, where multiple parameters have changed, this strategy should still be employed to improve the performance of the part, but it must be recognized that the chemical differences between 42A and the 101 will also have an impact on mechanical behavior for which revisions to thermal treatments may not compensate.

A more detailed analysis of the crystal phases present in these materials was conducted based on the peak fitting analysis. Specifically, it was first expected that the thermal history of the two parts may have resulted in differing amounts of the α_p and β_p phases, or residual γ phase. As represented by the data presented in figure 3, the data obtained from the samples were isotropic, which precludes the traditional analysis of the phases present by tilting the sample. Detailed analysis, however, was still possible by examining the data using multipeak fitting techniques and searching for the best fit based on the known crystal structures of nylon 6 6. First, the data

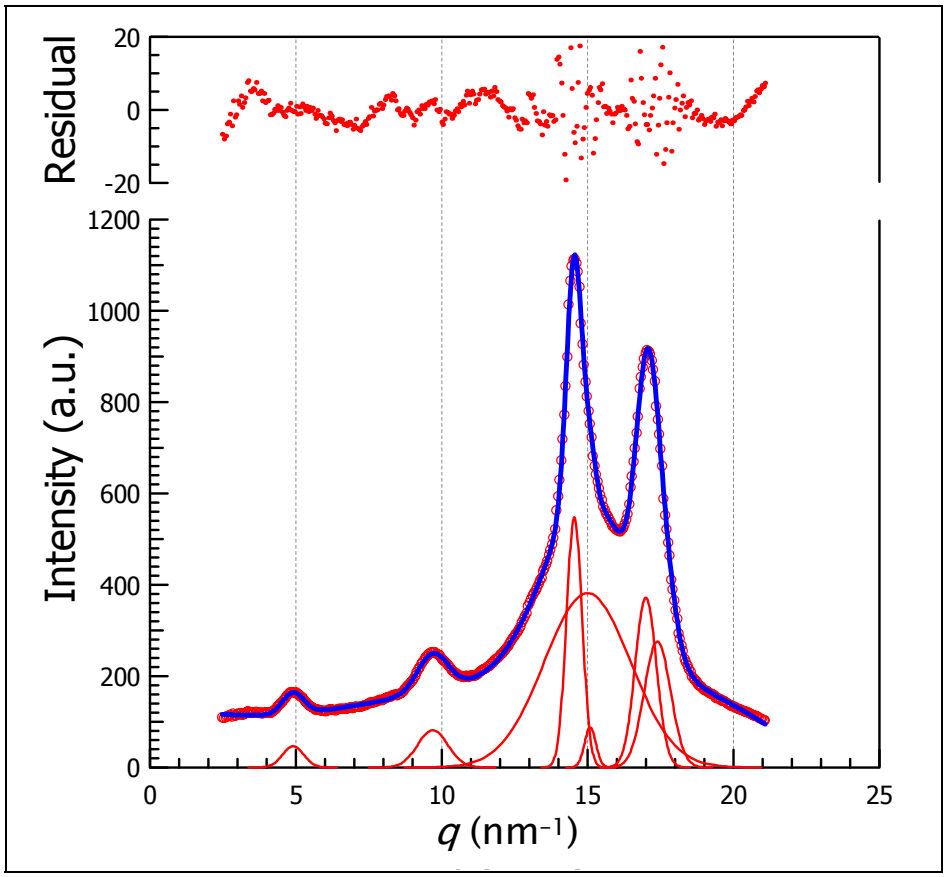

Figure 6. Graphical results of peak fitting analysis, showing WAXS data for 101 spot 1, fit data, and the seven individual components (as listed in table 3) that comprise the fit data. All peak shapes are Gaussian. The variation from the WAXS data of the fit is given as the residual component, indicating the quality of the fit.

Table 3. Peak fitting data generated using Igor Pro, Gaussian peak shapes, and a third-order polynomial background for sample 101 location 1.

Peak	***q*** **(nm^{-1})**	**Corresponding d Spacing (nm)**	**Amplitude (nm^{-1})**	**Width (nm^{-1})**
(001)	4.91	1.28	46.3	0.512
(002)	9.70	0.648	81.7	0.731
(100)	14.5	0.433	548	0.377
(010)	17.0	0.370	372	0.514
(110)	17.4	0.361	276	0.639
Residual γ phase peak	15.1	0.416	87.3	0.275
Amorphous halo	15.0	0.418	382	2.09

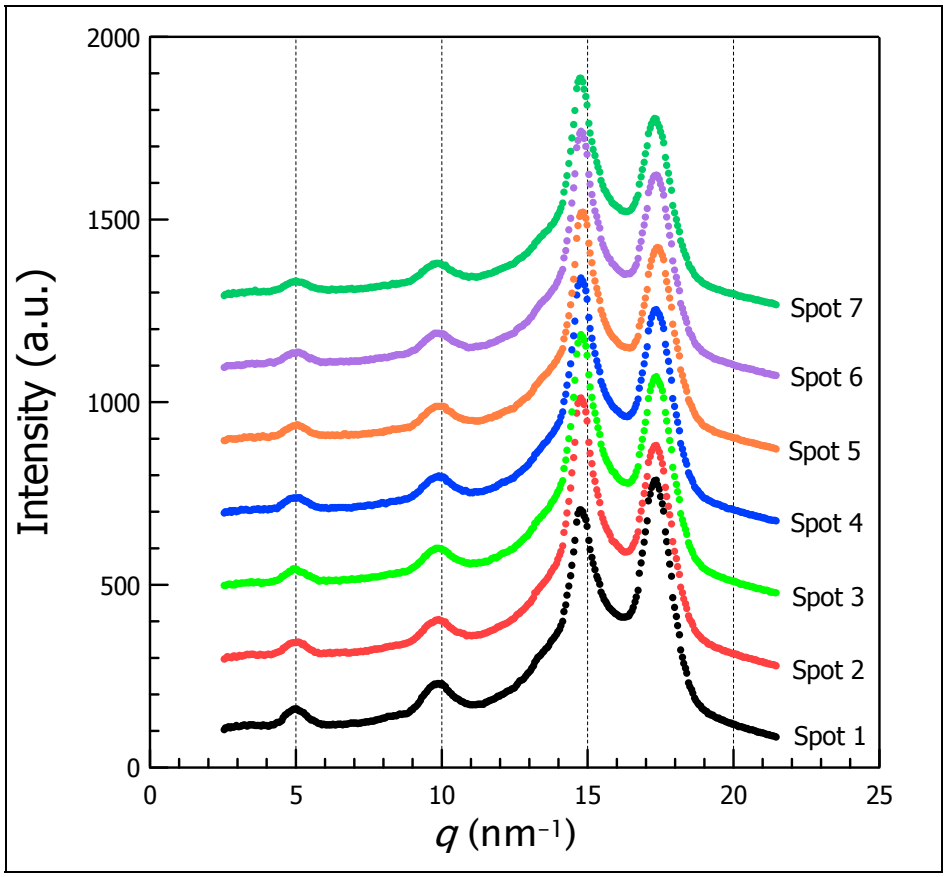

Figure 7. WAXS data for seven radial locations sectioned from the obturator manufactured from nylon 6 6 42A. The data are separated vertically for clarity. A significant difference in the relative intensities of the two characteristic reflections is noted between location 1 and the rest of the sample.

were fit with four peaks, one for each strong reflection, a single broad peak for amorphous content, and the third-order polynomial background function. These efforts resulted in fits in which the first characteristic nylon 6 6 reflection (14.5 nm^{-1}) matched the β_p phase, but the second characteristic peak (17.2 nm^{-1}) matched the α_p phase combination of (010) and (110). The (001) and (002) reflections corresponded well to an α_p phase material. Adding a second reflection to the fit, to account for the two reflections that contribute in either phase to the second characteristic reflection, improved the fit and resulted in peaks at 17.0 and 17.4 nm^{-1}, corresponding well to an all-α_p phase material. To account for a shoulder still apparent on the first characteristic reflection, occurring around the value of q where any residual γ phase would be expected to appear, a seventh peak was added to the fit. This further improved the fit, with a very small reflection appearing at 15.1 nm^{-1}, corresponding well to the idea that a trace of nonequilibrium γ phase is present in the samples. Further analysis did not reveal compelling evidence that any β_p phase is present in these materials, although the residuals from the peak fitting exercises being greatest around the characteristic peaks suggests that the fitting analysis is

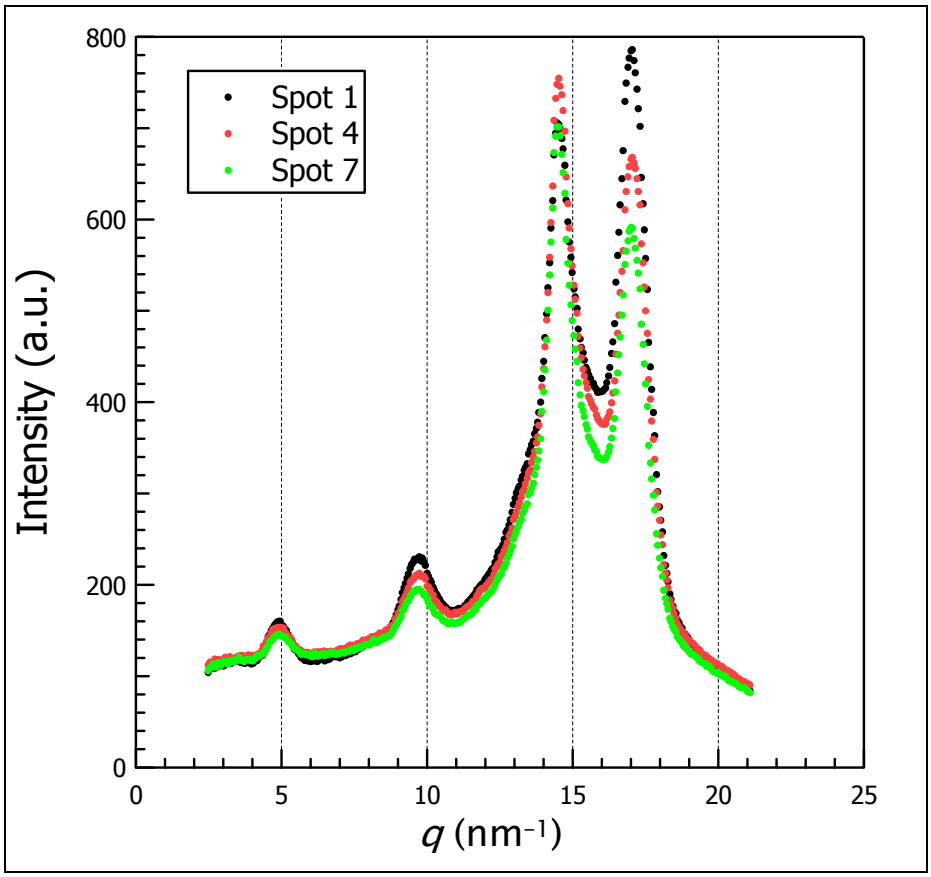

Figure 8. WAXS data from the three locations on the inner surface (1), center (4), and outer surface (7) of the obturator part manufactured using nylon 6 6 42A. Clearly there are significant variations in the morphology between these three locations in the part.

incomplete in some fashion. This may be a result of unascribed reflections in the fit, or it may be a result of discrepancies between Gaussian peak shapes and those in the data, which are likely not strictly Gaussian (*9*).

4. Conclusions

The purpose of this study was to examine two samples of commercial polyamide nylon 6 6, DuPont Zytel 42A and Zytel 101, for differences in morphology. The newer material, 42A, does not perform as well as the older material, 101, but is preferred due to availability. WAXS revealed that the materials were composed of isotropically oriented α_p phase sheets which formed lamellae. Evidence of a very small fraction of nonequilibrium γ phase material was found in both materials. No evidence of the β_p phase was seen. Where the 101 material was very uniform in morphology based on the WAXS data analysis, the morphology of 42A changed

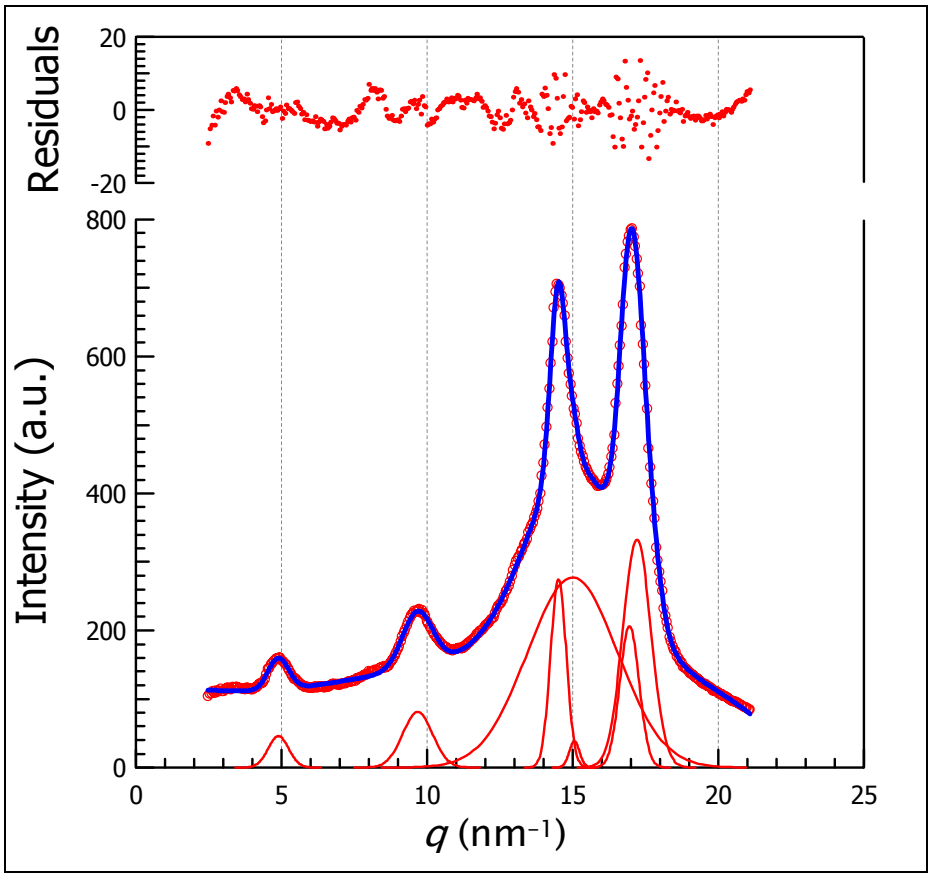

Figure 9. Peak fitting results for 42A location 1.

as a function of position within the part, as indicated by a change in the relative characteristic peak intensities moving radially through the sample. These changes indicated that the lamellae formed by stacks of α_p sheets are relatively short and wide near the inner surface of the part, changing to longer and more narrow near the outer surface of the part. This change most likely results from a change in the thermal history of the parts made from the 42A material from those made using the 101, although changes in other chemical and physical aspects of 42A relative to 101 must not be overlooked. The observed differences in morphology are expected to have a significant impact on mechanical properties. The critical difference between the two materials, upon first inspection, appears to be only the parameters and methods used in the annealing process. Therefore, a logical first step would be to revert to the oil-bath annealing process used for the 101 material, and then re-evaluate the performance of the 42A material. Under the current circumstances, an objective determination of the change in performance is not possible. Further studies of thermal processing effects could be conducted to optimize mechanical performance relative to annealing and cooling times.

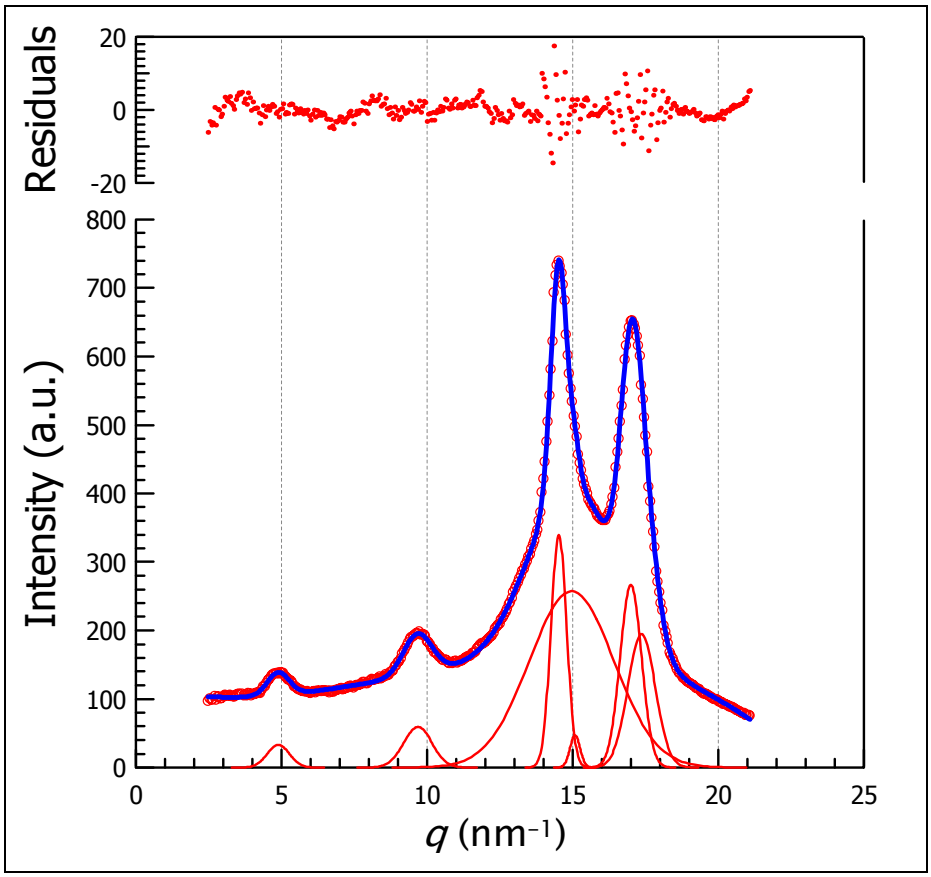

Figure 10. Peak fitting results for 42A location 4.

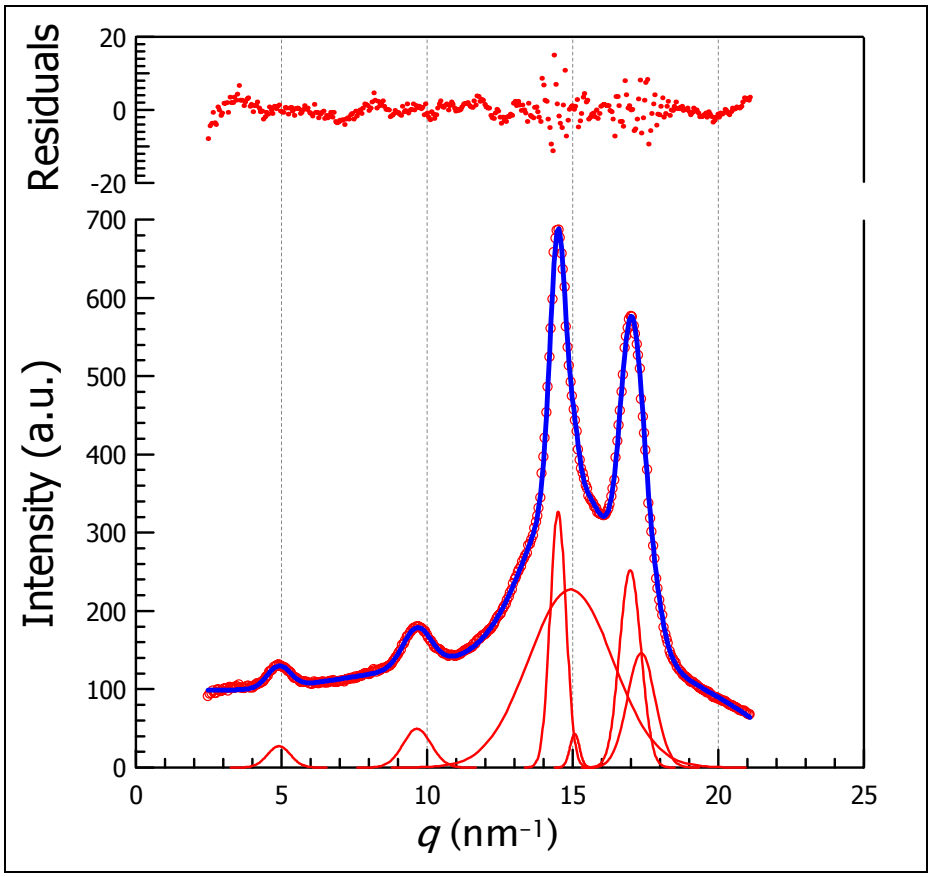

Figure 11. Peak fitting results for 42A location 7.

Table 4. Peak fit data calculated from WAXS data collected from material 42A at locations 1, 4, and 7, corresponding to the inner, center, and outer radial positions from the section taken from the part.

Reflection	42A Location 1				42A Location 4				42A Location 7			
	q (nm^{-1})	d (nm)	Width (nm^{-1})	Amplitude (a.u.)	*q* (nm^{-1})	d (nm)	Width (nm^{-1})	Amplitude (a.u.)	*q* (nm^{-1})	d (nm)	Width (nm^{-1})	Amplitude (a.u.)
(001)	4.89	1.28	0.495	45.9	4.89	1.28	0.531	33.1	4.91	1.30	0.557	27.1
(002)	9.67	0.650	0.725	80.8	9.68	0.649	0.694	59.1	9.65	0.651	0.685	49.4
(100)	14.5	0.433	0.382	274	14.5	0.433	0.379	339	14.5	0.433	0.384	327
(010)	16.9	0.372	0.469	206	17.0	0.370	0.521	267	17.0	0.370	0.517	252
(110)	17.2	0.365	0.680	333	17.4	0.361	0.665	195	17.4	0.361	0.677	146
γ phase	15.1	0.416	0.248	38.3	15.1	0.416	0.240	47.3	15.1	0.416	0.229	42.9
Amorphous halo	15.0	0.419	2.19	277	15.0	0.419	2.05	257	14.9	0.422	2.04	228

5. References

1. Bunn, C. W.; Garner, E. V. *Proceedings of the Royal Society of London Series A. Mathematical and Physical Sciences* **1947**, *189*, 39.
2. Starkweather, H. W.; Johnson, D. R.; Whitney, J. F. Part A-General Papers. *Journal of Polymer Science* **1963**, *1*, 715.
3. Jones, N. A.; Atkins, E. D. T.; Hill, M. J. Part B-Polymer Physics. *Journal of Polymer Science* **2000**, *38*, 1209–1221.
4. Brill, R. Z. *Physik Chem*. **1943**, *61*, 1353.
5. Hirschinger, J.; Miura, H.; Gardner, K. H.; English, A. D. *Macromolecules* **1990**, *23*, 2153–2169.
6. Pfluger, R. In *Polymer Handbook*, 2nd ed.; Brandrup, J.; Immergut, E. H., Eds.; John Wiley and Sons: New York, 1975; pp V79–V66.
7. Ladd, M. F. C.; Palmer, R. A. *Structure Determination by X-ray Crystallography*, 3rd ed.; Plenum Press: New York, 1993.
8. Cullity, B. D. *Elements of X-ray Diffraction*, 2nd ed.; Addison-Wesley Publishing Company, Inc.: Reading, MA, 1978.
9. Roe, R. J. *Methods of X-ray and Neutron Scattering in Polymer Science*; Oxford University Press: New York, 2000.

NO. OF COPIES	ORGANIZATION
1 (PDF Only)	DEFENSE TECHNICAL INFORMATION CTR DTIC OCA 8725 JOHN J KINGMAN RD STE 0944 FT BELVOIR VA 22060-6218
1	COMMANDING GENERAL US ARMY MATERIEL CMD AMCRDA TF 5001 EISENHOWER AVE ALEXANDRIA VA 22333-0001
1	INST FOR ADVNCD TCHNLGY THE UNIV OF TEXAS AT AUSTIN 3925 W BRAKER LN STE 400 AUSTIN TX 78759-5316
1	US MILITARY ACADEMY MATH SCI CTR EXCELLENCE MADN MATH THAYER HALL WEST POINT NY 10996-1786
1	DIRECTOR US ARMY RESEARCH LAB AMSRD ARL CS IS R 2800 POWDER MILL RD ADELPHI MD 20783-1197
3	DIRECTOR US ARMY RESEARCH LAB AMSRD ARL CI OK TL 2800 POWDER MILL RD ADELPHI MD 20783-1197
3	DIRECTOR US ARMY RESEARCH LAB AMSRD ARL CS IS T 2800 POWDER MILL RD ADELPHI MD 20783-1197

NO. OF COPIES	ORGANIZATION
	ABERDEEN PROVING GROUND
1	DIR USARL AMSRD ARL CI OK TP (BLDG 4600)

NO. OF
COPIES ORGANIZATION

ABERDEEN PROVING GROUND

6 AMSRD ARL WM MA
F BEYER (3 CPS)
AMSRD ARL WM MD
P DEHAUER (3 CPS)

INTENTIONALLY LEFT BLANK.